ARTICLE
Journal of Cellular Biochemistry 113:985–996 (2012)

Journal of Cellular Biochemistry

The DEAD-Box RNA Helicase DDX3 Interacts With DDX5, Co-Localizes With it in the Cytoplasm During the G_2/M Phase of the Cycle, and Affects Its Shuttling During mRNP Export

Yeo-Jin Choi and Seong-Gene Lee*

Department of Biotechnology, Bioenergy Research Center, Chonnam National University, Gwangju 500-757, South Korea

ABSTRACT

DDX3 is involved in RNA transport, translational control, proliferation of RNA viruses, and cancer progression. From yeast two-hybrid screening using the C-terminal region of DDX3 as a bait, the DEAD-box RNA helicase DDX5 was cloned. In immunofluorescence analysis, DDX3 and DDX5 were mainly co-localized in the cytoplasm. Interestingly, cytoplasmic levels of DDX5 increased in the G_2/M phase and consequently protein–protein interaction also increased in the cytoplasmic fraction. DDX3 was highly phosphorylated at its serine, threonine, and tyrosine residues in the steady state, but not phosphorylated at the serine residue(s) in the G_2/M phase. DDX5 was less phosphorylated in the G_1/S phase; however, it was highly phosphorylated at serine, threonine, and tyrosine residues in the G_2/M phase. PP2A treatment of the cytoplasmic lysate from G_2/M phase cells positively affected the interaction between DDX3 and DDX5, whereas, PTP1B treatment did not. In an analysis involving recombinant His-DDX3 and His-DDX5, PP2A pretreatment of His-DDX5 increased the interaction with endogenous DDX3, and vice versa. Furthermore, the results of GST pull-down experiments support the conclusion that dephosphorylation of serine and/or threonine residues in both proteins enhanced protein–protein interactions. UV cross-linking experiments showed that DDX3 and DDX5 are involved in mRNP export. Additionally, DDX3 knockdown blocked the shuttling of DDX5 to the nucleus. These data demonstrate a novel interaction between DDX3 and DDX5 through the phosphorylation of both proteins, especially in the G_2/M phase, and suggest a novel combined mechanism of action, involving RNP remodeling and splicing, for DEAD-box RNA helicases involved in mRNP export. J. Cell. Biochem. 113: 985–996, 2012.

KEY WORDS: DEAD-BOX; DDX3; DDX5; PHOSPHORYLATION; PROTEIN–PROTEIN INTERACTION; mRNP EXPORT

DEAD-box RNA helicases are characterized by nine conserved motifs, and display RNA-dependent ATPase and ATP-dependent RNA helicase activities. DEAD-box proteins play important roles in RNA metabolism; they are very specific and do not compensate each other's activities. DEAD-box proteins have been reported to be necessary for, or involved in, many different processes of RNA metabolism. In eukaryotic cells, in particular, these processes range from transcription to RNA degradation, and include pre-mRNA splicing, mRNA export, ribosome biogenesis, translation initiation, and gene expression in organelles [Linder, 2006].

DDX3 is a nucleo-cytoplasmic shuttling protein with RNA-dependent ATPase/helicase activity [You et al., 1999; Yedavalli et al., 2004]. Although the precise biological function of DDX3 remains elusive, it may be involved in many cellular processes, including translational control, mRNA migration, cell cycle control, viral replication, and tumor suppression [Rosner and Rinkevich, 2007]. Several studies have described DDX3 as a protein that constantly shuttles between the cytoplasm and the nucleus, with its export from the nucleus being mediated by the export shuttle protein CRM1 [Yedavalli et al., 2004; Schröder et al., 2008]. Recently, DDX3 was also shown to be exported via the TAP-dependent export pathway, which normally mediates the nuclear export of mRNAs [Lai et al., 2008]. DDX3 has been isolated from RNA-transporting granules, indicating a role in mRNA migration [Kanai et al., 2004], and has been shown to associate with functional

Additional Supporting Information may be found in the online version of this article.

Grant sponsor: The Basic Research Program of the Korea Science & Engineering Foundation; Grant number: R04-2003-000-10126-0; Grant sponsor: Priority Research Centers Program through the National Research Foundation of Korea (NRF); Grant number: 2011-0018393.

*Correspondence to: Prof. Seong-Gene Lee, Department of Biotechnology, Chonnam National University, 300 Yongbong-Dong, Buk-Gu, Gwangju 500-757, Korea. E-mail: sglee3@chonnam.ac.kr

Received 1 July 2011; Accepted 18 October 2011 • DOI 10.1002/jcb.23428 • © 2011 Wiley Periodicals, Inc.
Published online 27 October 2011 in Wiley Online Library (wileyonlinelibrary.com).

spliceosomes, indicating a role in RNA splicing [Zhou et al., 2002]. Composition analysis, performed using spliced and unspliced messenger ribonucleoprotein (mRNPs), showed that DDX3 associates with mRNP proteins and interacts with mRNAs during splicing via the exon junction complex [Merz et al., 2007]. Furthermore, DDX3 is required not only for HIV Rev-RRE export [Yedavalli et al., 2004], but also for hepatitis C virus (HCV) RNA replication [Arimui et al., 2007], suggesting a role in the life cycle or pathogenesis of certain viruses.

In this study, we identified the protein-binding partners of DDX3 to understand the biological function of DDX3. Using yeast two-hybrid screening with the C-terminal region (aa 501–662) of DDX3 as bait, we screened recombinant DEAD-box RNA helicase DDX5 (also known as p68) for an interaction. DDX5, a well-known DEAD-box RNA helicase involved in various biological processes, such as transcriptional control, nuclear mRNA export, the pathogenesis of the HCV, cancer progression, RNA splicing, and the microRNA pathway [Endoh et al., 1999; Zhou et al., 2002; Goh et al., 2004; Yang et al., 2005; Salzman et al., 2007], as an interacting protein. DDX5 is known to have an interacting partner, DDX17, which is a DEAD-box RNA helicase. These two proteins share 92% homology within their central helicase domains. Both proteins possess RNA helicase activity and are involved in splicing, but also function in the regulation of gene transcription [Ogilvie et al., 2003; Fuller-Pace, 2006]. DDX3 is another partner of DDX5, and we need to understand the possible role of protein–protein interaction between these two DEAD-box RNA helicases. DDX3 and DDX5 have nine helicase domains and show only 60% homology within these highly conserved domains. DDX3 and DDX5 have been found to be co-involved in RNA splicing, mRNP metabolism [Fuller-Pace, 2006; Merz et al., 2007], Staufen-containing RNA-transporting granules of antiretroviral factor APOBEC3G [Chiu et al., 2006], and hepatitis C viral replication [Goh et al., 2004; Arimui et al., 2007]. This study suggests that DDX3 and DDX5 may play a common role in mRNP metabolism and RNA viral replication via direct interaction. To characterize the protein–protein interaction, we raised new antibodies to DDX3 and DDX5 and analyzed the interacting region between both proteins. Immunofluorescence (IF) and immunoprecipitation (IP) analyses suggested that both proteins co-localized in the cytoplasmic fraction. Depending on the cell cycle, DDX3 localization was altered. The protein–protein interaction was rapidly increased in the G_2/M phase. During the G_2/M phase, phosphorylation of DDX3 was decreased, whereas, the phosphorylation of DDX5 was increased, compared with the G_1/S phase. To investigate the effects of the cell cycle and the phosphorylation of DDX3 and DDX5 on their interaction, IP analysis was performed with anti-DDX3 antibody after treatment with PP2A and/or PTP1B. From this experiment, we found that phosphorylation at serine/threonine residue(s) of both DDX3 and DDX5 affected the protein–protein interaction. Furthermore, UV cross-linking experiments showed that both RNA helicase proteins were involved in mRNP metabolism and that, notably, DDX3 affected the shuttling of DDX5 to the nucleus. These data demonstrate a novel interaction between DEAD-box RNA helicase DDX3 and DDX5, which is dependent on the phosphorylation of both proteins (especially in the G_2/M phase). This finding also suggests a novel combined mechanism of action involving RNP remodeling and splicing and DEAD-box RNA helicase involvement in mRNP export.

MATERIALS AND METHODS

YEAST TWO-HYBRID SCREENING

All yeast strains and plasmids for two-hybrid screening (Matchmaker two-hybrid system) were obtained from Clontech (Palo Alto, CA). The C-terminal region corresponding to amino acid residues 501–662 (161 aa) of DDX3 was used to screen a library (5×10^5 independent clones) of human fetal brain cDNAs, each fused to the GAL4 activation domain in the pACT2 vector. The yeast strain AH109 was used as the host, and cells positive for growth on selective medium (−Ade/−His/−Leu/−Trp) were examined for α-galactosidase activity using 5-bromo-4-chloro-3-indolyl alpha-D-galactopyranoside (Sigma–Aldrich, St. Louis, MO). Positive interactions were confirmed by reintroducing cDNA (and subcloned derivatives) of retrieved clones into yeast AH109 and performing control crosses with yeast harboring the pGBKT7-DDX3 or pGBKT7-DDX3 deleted constructs. To characterize the interacting regions between DDX3 with DDX5, pGBKT7/DDX3 deleted constructs were used in two-hybrid experiments. To confirm the interacting region between DDX3 and DDX5, deleted constructs of DDX5 and full-length DDX5 (kindly gifted by Prof. Fuller-Pace, University of Dundee) cloned into the pGADT7 plasmid were used.

ANTIBODIES

To generate polyclonal antibodies, bacterially expressed DDX3 and DDX5 were immunized in rabbits and rats. To confirm the constructed antibodies, commercial anti-DDX3 and anti-DDX5 antibodies were purchased from Novus Biologicals (Littleton, CO). Anti-nucleophosmin (NPM) was purchased from Zymed Laboratories (South San Francisco, CA) and anti-β actin and α-tubulin antibodies were purchased from BioVision (Mountain View, CA). Anti-phospho serine (16B4) and anti-phospho threonine (14B3) antibodies were purchased from Calbiochem (San Diego, CA) and anti-phospho tyrosine (PY20) antibody was purchased from Santa Cruz (Santa Cruz, CA). Alexa-fluor 488 and 546 antibodies were purchased from Molecular Probes (Carlsbad, CA).

PROTEIN EXPRESSION AND PURIFICATION

In-frame fusion of the recombinant full-length DDX3 was constructed using the pCold vector (Takara Bio Inc, Ostu, Shiga) for bacterial expression as an amino-terminal $(His)_6$-tagged protein. DDX5 was cloned into the pET28a (EMD Chemicals, Darmstadt, Germany) vector and expressed in BL21 codonplus (Stratagene, La Jolla, CA). The fusion protein, His-DDX3, was induced with 1 mM isopropyl β-D-1-thiogalactopyranoside (IPTG) at 15–20°C for 20 h, harvested, sonicated, and then the soluble fraction was retained after centrifugation. His-DDX3 and His-DDX5 were purified through a Ni-NTA His-Bind resin column (Novagen, Gibbstown, NJ).

PREPARATION OF PROTEIN FROM CELLS AND IMMUNOBLOTTING

Cell lysates prepared in lysis buffer (130 mM NaCl, 10 mM Tris–Cl, pH 7.4, 5 mM EDTA, and 1% Triton X-100) were used to prepare control lysates for immunoblotting. The cultured cells were lysed in

lysis buffer containing 10 mM phenylmethanesulphonylfluoride (PMSF) and a complete protease inhibitor cocktail (Roche Molecular Biochemicals, Mannheim, Germany). Lysates were sonicated briefly and cleared by centrifugation at $16,000 \times g$ for 5 min. To isolate the nuclear and cytoplasmic fractions, 1×10^7 HeLa cells were incubated in 200 μl hypotonic buffer (10 mM HEPES, pH 7.9, 3 mM $MgCl_2$, 10 mM KCl, 1 mM dithiothreitol (DTT), and 0.5% Igepal) with 1 mM PMSF and a cocktail of protease inhibitors for 10 min on ice. The cells were centrifuged at $3,800 \times g$ for 10 min at 4°C and the supernatant was saved as the cytoplasmic fraction. The pellets were suspended with 200 μl nuclear extract buffer (500 mM NaCl, 10 mM Tris–Cl, pH 7.5, 0.5 mM EDTA, 0.5 mM EGTA, 1.5 mM $MgCl_2$, 1 mM DTT, and 2.5% glycerol) and incubated on ice for 10 min, and then centrifuged at $16,000 \times g$ for 10 min at 4°C. The supernatants were saved as the nuclear fraction for IP. Cells were suspended in 200 μl lysis buffer, incubated for 10 min on ice, and centrifuged at $16,000 \times g$ at 4°C for 10 min after sonication. The supernatants were saved and used as whole lysates for further analysis and as a control. Sample protein content was determined using the Bio-Rad protein assay reagent (Sigma–Aldrich), with bovine serum albumin as the standard. Equal amounts of protein (30 μg/lane) were resolved by 10–12% SDS–PAGE and transferred onto a nitrocellulose membrane. The membrane was then washed with Tris-buffered saline (10 mM Tris and 150 mM NaCl) containing 0.05% Tween 20 (TBST), and blocked with TBST containing 5% non-fat dry milk powder. The membrane was incubated with the respective specific antibodies [DDX3 (1:1,000), DDX5 (1:1,000), phospho-Ser (1:300), phospho-Thr (1:300), phospho-Tyr (1:1,000), NPM (1:1,000), α-tubulin (1:1,000), and β-actin (1:1,000)]. The membrane was next incubated with the appropriate secondary antibody coupled to horseradish peroxidase, and developed with ECL Western blot detection reagents (Amersham Pharmacia Biotech, Piscataway, NJ).

IMMUNOPRECIPITATION (IP)

The cytoplasmic lysates were purified from G_1/S or G_2/M arrested cells, and IP analysis was performed with 1.5 mg of protein lysate and 5 μg anti-DDX3 or DDX5 polyclonal antibody in a total volume of 500 μl of lysis buffer, a complete protease inhibitor cocktail, and 20 μl of protein A/G Sepharose beads (Calbiochem) overnight at 4°C. To evaluate the effect of phosphorylation on the DDX3/DDX5 interaction, 1.5 mg of protein lysate or bacterially expressed His-DDX3 or His-DDX5 (40 μg) was treated with phosphatases, PP2A, and/or PTP1B, and then IP analysis was performed with anti-DDX3 or anti-His antibodies. Immunoprecipitated proteins were separated by SDS–PAGE and immunoblotted with specific antibodies, as described above. For immunoblotting of the same membrane with different antibodies, bound antibody was removed by incubating the membrane in 50 mM Tris–HCl, pH 6.8, 2% SDS, and 100 mM β-mercaptoethanol for 15 min at room temperature, followed by extensive washing in PBS-T (0.1% Tween 20 in PBS).

IMMUNOFLUORESCENCE (IF) STAINING

To analyze the intracellular localization of DDX3 and DDX5, HeLa cells were grown as polarized monolayers on 12 mm tissue culture inserts (Nunc, Rochester, NY). Four percent formaldehyde-fixed cells were stained by incubating them with the primary antibodies (rabbit polyclonal anti-DDX3 antibody and rat polyclonal anti-DDX5 antibody) diluted to 1:50 in blocking buffer (PBS with 5% BSA) for 2 h at room temperature. The cells were rinsed with PBS following blocking buffer incubation, and exposed to the secondary antibodies (1:1,000; Alexa 488 for DDX5 and Alexa 546 for DDX3) for 2 h at room temperature. The nucleus of the cell was stained with TO-PRO-3 (Molecular Probes). The stained cells were mounted and imaged using a laser confocal scanning microscope (Leica, Heidelberg, Germany).

CELL SYNCHRONIZATION AND FLOW CYTOMETRY ANALYSIS

To analyze the cell cycle-dependent phosphorylation and localization of DDX3 and DDX5, HeLa cells were treated with 2 mM hydroxyurea (Sigma–Aldrich) twice for 12 h to reach the G_1/S phase. For G_2/M phase arrest, HeLa cells were treated with 600 ng/ml nocodazole (Sigma–Aldrich) until all cells became mitotic. The synchronized cells were analyzed by flow cytometry using FACSCalibar (BD Biosciences, San Jose, CA).

PHOSPHATASE TREATMENT

A total of 1.5 mg lysate or 40 μg bacterially expressed His-DDX3 and His-DDX5 were treated with PP2A (0.12 U/mg) and PTP1B (0.19 U/mg) (Sigma–Aldrich) for 2 h at 30°C. After treatment, the lysates were immunoprecipitated with anti-DDX3 antibody and immunoblotted with anti-DDX3 and anti-DDX5 antibodies, or anti-His antibody, respectively.

GST PULL-DOWNS

DDX3 cDNA was cloned in the vector pcDNA-Myc which allows expression of c-Myc-tagged proteins in mammalian cells. Myc-DDX3 (prepared in this study) and GST-tagged DDX5 [Ogilvie et al., 2003] were transfected into HEK293 cells for 24 h and cells were harvested and lyzed in lysis buffer. The lysates were treated with 0.1 μM calyculin A (Sigma–Aldrich) for 30 min on ice and followed by 0.12 U/mg PP2A for 2 h at 30°C. After incubation, GST-tagged DDX5 was purified on glutathione beads using standard conditions and immunoblotted with anti-Myc and anti-DDX5 antibodies, respectively.

UV-INDUCED CROSS-LINK OF RNA TO PROTEIN AND mRNA AFFINITY CHROMATOGRAPHY

The in vivo UV cross-linking process was described in elsewhere [Piñol-Roma et al., 1989]. Irradiation was performed using a UV cross-linker Viber lourmat BLX-254 (Marne le Valle, France). Total cell lysate or subcellular fractions of HEK293 were subsequently prepared as described above. The fractions were heated for 5 min at 65°C in the presence of 0.5% SDS and 1% β-mercaptoethanol. After chilling on ice, LiCl was added to the fractions a final concentration of 0.5 M. Oligo(dT)-cellulose beads (Sigma–Aldrich) were previously swelled and equilibrated in binding buffer (10 mM Tris–Cl, pH 7.4, 1 mM EDTA, 0.5% SDS, and 0.5 M LiCl). The fractions were incubated with beads at room temperature for 30 min. Subsequently, RNP complexes were precipitated with 0.2 M of LiCl and three volumes of ethanol at −20°C overnignt. After digestion with 50 μg/ml RNase A for 1 h at 37°C, RNA-binding proteins were precipitated

with 10% trichloroacetic acid and analyzed by immunoblotting. To verify the effect of DDX3 on the role of DDX5 in mRNP export, shDDX3 was constructed. The pRNAT-H1.1/Adeno (GenScript, Piscataway, NJ) vector was used to express short hairpin RNAs (shRNAs) targeting human DDX3 (NM_001356, nts 2,800–2,818). After transfection of shDDX3 into HEK293 cells, UV cross-linking experiment was carried out as described above.

RESULTS

DDX3 INTERACTS WITH DDX5

For the yeast two-hybrid screening, we used the C-terminal region of DDX3 as the bait to exclude the highly homologous helicase domain region and to find a molecule that interacted specifically with DDX3. We cloned a partial cDNA of DDX5 (aa 76–614), a DEAD-box RNA helicase family protein. Full-length DDX3 and $DDX3_{415-662}$, which contains helicase motifs IV–VI and a Ser/Gly-rich region, interacted with DDX5 (Fig. 1). However, $DDX3_{1-420}$, which contains the Q motif and helicase motifs I–III, did not interact with DDX5. Interestingly, DDX3 did interact with itself and could form a homodimer; however, the homodimer was not demonstrated in vivo. DDX5 and $DDX5_{373-614}$, which contain helicase motifs V and VI, interacted with DDX3, whereas, $DDX5_{1-387}$, which contains the Q motif and helicase motifs I–IV, did not. DDX5 formed a strong homodimer, as described previously [Ogilvie et al., 2003].

To analyze the interaction between DDX3 and DDX5, we raised rabbit and rat polyclonal antibodies to bacterially expressed His-DDX3 and His-DDX5, respectively. The anti-DDX3 and anti-DDX5 antibodies detected 73 and 68 kDa proteins, respectively. In IP analysis, His-DDX3 co-immunoprecipitated with His-DDX5 and vice versa (Fig. 2A). In HeLa cells, IP analysis was performed with rabbit IgG and anti-DDX3 or rat IgG and anti-DDX5 (Fig. 2B). Each antibody detected specific target protein and did not show non-specific interaction with cellular proteins. DDX3 was detected predominantly in the cytoplasmic fraction, whereas, DDX5 was detected predominantly in the nuclear fraction of HeLa cell lysates (Fig. 2C). When IP analysis was performed with an anti-DDX3 antibody, DDX5 was more strongly immunoprecipitated in the

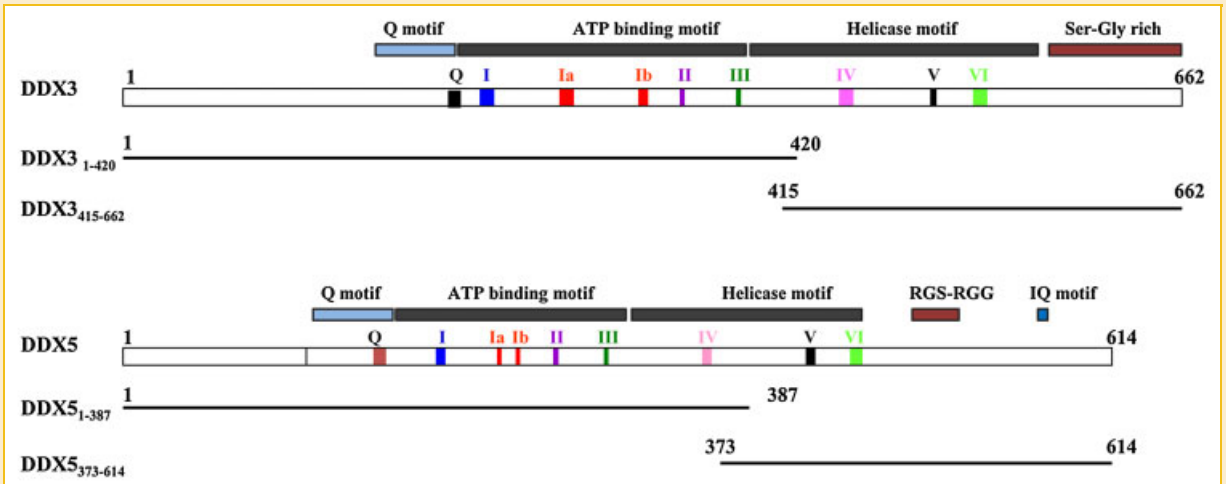

pGADT7 / pGBKT7	DDX5	DDX3
$DDX3_{1-420}$	–	–
$DDX3_{415-662}$	+++	++
DDX3	++	+
$DDX5_{1-387}$	ND	–
$DDX5_{373-614}$	ND	+++
DDX5	+++	++

Fig. 1. Interaction of DDX3 and DDX5 in a yeast two-hybrid system. In each case, deletion derivatives were tested for interactions with respective full-length partners in a yeast two-hybrid system. cDNAs encoding DDX3 and DDX5 were cloned into yeast two-hybrid vectors such that they were fused to either the DNA-binding domain (pGBKT7) or transcriptional activation domain (pGADT7) of GAL4 and tested for interactions in a standard yeast two-hybrid assay. The numbers included in each of the deletions indicate amino acids. Nine conserved helicase motifs are shown as colored letters. The Q motif and serine-rich and glycine-rich regions are indicated at the top of the map. +++, strong interaction (100% blue colonies); ++, weak interaction (<50% blue colonies); +, weak interaction (<10% blue colonies); –, no interaction (no blue colonies); ND, not determined. [Color figure can be seen in the online version of this article, available at http://wileyonlinelibrary.com/journal/jcb]

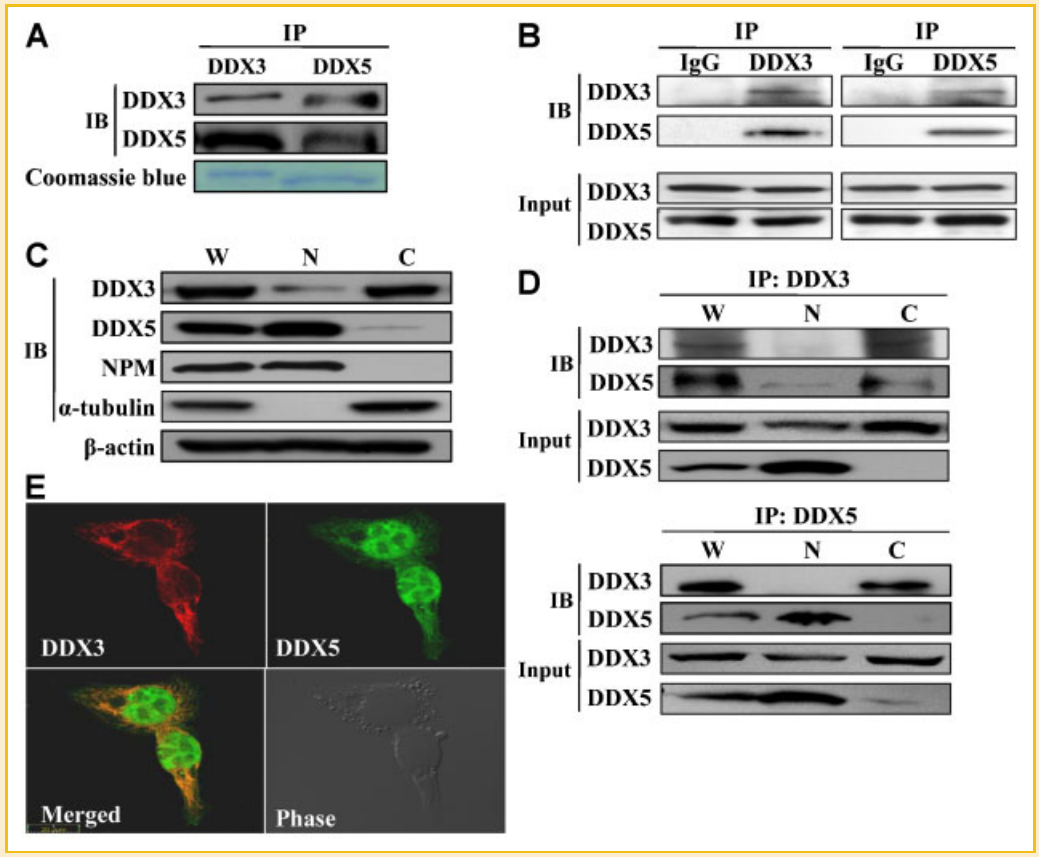

Fig. 2. Interaction of DDX3 and DDX5 in vitro and in vivo. A: Recombinant DDX3 and DDX5 were purified, immunoprecipitated, and then immunoblotting with anti-DDX5 and anti-DDX3 antibodies. B: Proteins from HeLa cell lysates were immunoprecipitated with anti-DDX3 antibody and rabbit IgG or anti-DDX5 antibody and rat IgG, and then immunoblotted with anti-DDX3 and anti-DDX5 antibodies. C: Proteins from HeLa cell lysates were immunoblotted with anti-DDX5 and anti-DDX3 antibodies. W, whole cell lysate; N, nuclear fraction; C, cytoplasmic fraction. Nuclear and cytoplasmic purifications were verified with anti-NPM and anti-α-tubulin antibodies. Normalization was performed with an anti-β actin antibody. D: Proteins from HeLa cell lysates were immunoprecipitated with an anti-DDX3 or an anti-DDX5 antibody and then immunoblotted with anti-DDX3 and anti-DDX5 antibodies. E: Localization of DDX3 and DDX5 in HepG2 cells determined by IF. The relative localization of proteins was determined by labeling, with appropriate secondary antibodies conjugated to Alexa Fluor 546 (red) and Alexa Fluor 488 (green) being used for DDX3 and DDX5, respectively. [Color figure can be seen in the online version of this article, available at http://wileyonlinelibrary.com/journal/jcb]

cytoplasmic fraction compared to the nuclear fraction (Fig. 2D). Using an anti-DDX5 antibody, DDX3 was more strongly immunoprecipitated in the cytoplasmic fraction than the nuclear fraction, even though DDX5 itself was predominantly localized in the nuclear fraction. In IF staining, DDX3 was primarily localized in the cytoplasm and in the speckled region of the nuclear membrane; DDX5 was localized predominantly in the nucleus and weakly dispersed in the cytoplasm (Fig. 2E). When the two signals were merged, co-localization appeared in the cytoplasm and this result matched the IP analysis.

ANALYSIS OF THE PHOSPHORYLATION PATTERNS OF DDX3 AND DDX5 DURING THE CELL CYCLE

The phosphorylation patterns of both RNA helicase proteins were analyzed using anti-phospho-serine, -threonine, and -tyrosine antibodies. As shown in Figure 3A, bacterially expressed recombinant DDX3 and DDX5 were highly phosphorylated at serine and threonine residues and relatively weakly phosphorylated at tyrosine residues. In HeLa cells, cytoplasmic DDX3 was phosphorylated at serine, threonine, and tyrosine residues. DDX5 immunoprecipitated from the cytoplasm was also phosphorylated at threonine and tyrosine residues, but only weakly at serine residues (Fig. 3B). To examine the interaction between DDX3 and DDX5 during the cell cycle, HeLa cells were arrested at the G_1/S and G_2/M phases and the nuclear and cytoplasmic fractions were prepared and immunoblotted with anti-DDX3 and anti-DDX5 antibodies, respectively (Fig. 3C). During the G_1/S phase, the cytoplasmic DDX3 level was 2–3-fold higher than the nuclear DDX3 level. However, the cytoplasmic DDX3 level was 0.53-fold lower during the G_2/M phase than during the G_1/S phase. The level of nuclear DDX3 did not differ between the G_1/S phase and the G_2/M phase. Interestingly, DDX5 was mostly localized in the nucleus and cytoplasmic DDX5 was detected at very low levels. However, cytoplasmic DDX5 rapidly increased during the G_2/M phase (Fig. 3C). To understand the association between protein levels and phosphorylation status of the two proteins, HeLa cells were arrested in the G_1/S and G_2/M phases and IP analysis with an anti-DDX3 antibody was followed by immunoblotting with anti-phospho antibodies (Fig. 3D). As shown

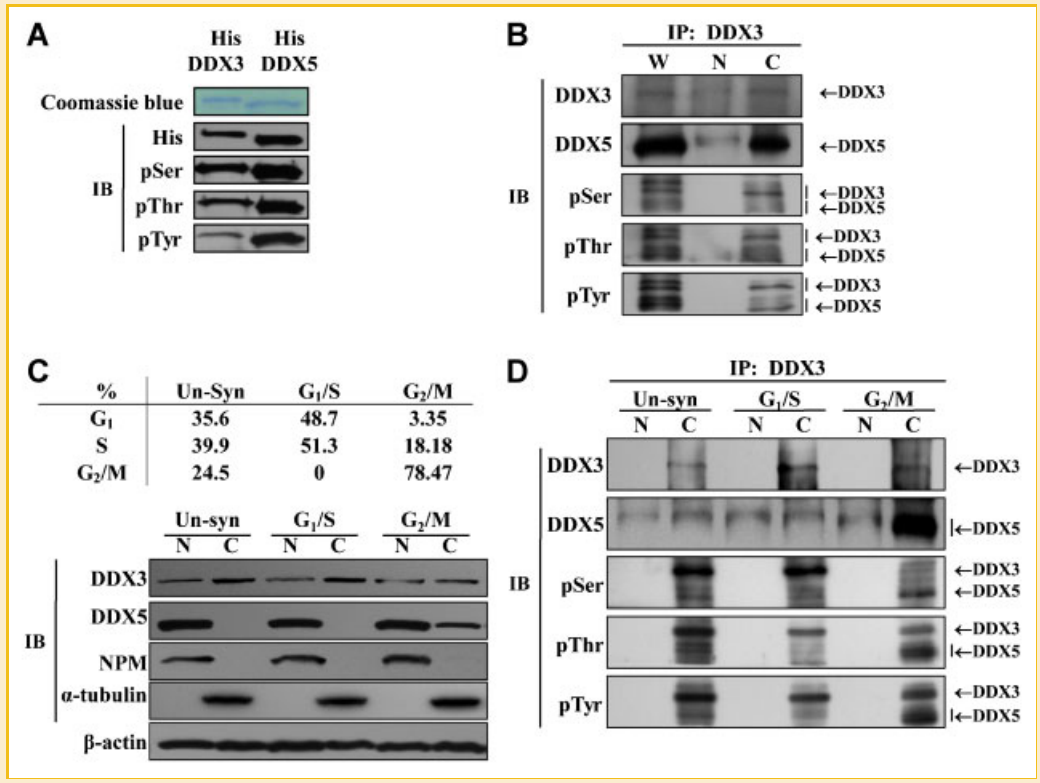

Fig. 3. Phosphorylation analysis of DDX3 and DDX5. A: Recombinant DDX3 and DDX5 were immunoblotted with anti-pSer, -pThr, and -pTyr antibodies. B: Proteins from HeLa cell lysates were immunoprecipitated with an anti-DDX3 antibody and then immunoblotted with anti-DDX3, -DDX5, -pSer, -pThr, and -pTyr antibodies. W, whole cell lysate; N, nuclear fraction; C, cytoplasmic fraction. C: HeLa cells were synchronized through treatment with 2 mM hydroxyurea twice for 12 h to reach the G_1/S phase. For G_2/M phase arrest, HeLa cells were treated with 600 ng/ml nocodazole until all cells became mitotic. To confirm cell cycle arrest, flow cytometry analysis was carried out. Lysates from cells in the G_1/S and G_2/M phases were immunoblotted with anti-DDX3 and anti-DDX5 antibodies. Nuclear and cytoplasmic purifications were verified with anti-NPM and anti-α-tubulin antibodies. Normalization was performed with an anti-β actin antibody. D: Lysates from cells in the G_1/S and G_2/M phases were subjected to IP with an anti-DDX3 antibody and then immunoblotting with anti-DDX3, -DDX5, -pSer, -pThr, and -pTyr antibodies. N, nuclear fraction; C, cytoplasmic fraction; Un-syn, unsynchronized. [Color figure can be seen in the online version of this article, available at http://wileyonlinelibrary.com/journal/jcb]

previously, the levels of immunoprecipitated DDX5 were the same in both the cytoplasmic and nuclear lysates during the G_1/S phase. However, the amount of DDX5 immunoprecipitated from the cytoplasm of cells in the G_2/M phase was much higher than that obtained from the cytoplasm of cells in the G_1/S phase (Fig. 3D). In the G_1/S phase, cytoplasmic DDX3 was highly phosphorylated at serine, threonine, and tyrosine residues, whereas, immunoprecipitated DDX5 was weakly phosphorylated at these three amino acids. While pSer-DDX3 level was much lower in the G_2/M phase compared with the G_1/S phase, pThr-DDX3 and pTyr-DDX3 levels did not change; however, levels of phosphorylated DDX5, especially pThr-DDX5 and pTyr-DDX5, increased greatly in the G_2/M phase.

CELL CYCLE-DEPENDENT LOCALIZATION OF DDX3 AND DDX5

HeLa cells were synchronized in the G_0 stage through serum-starvation for 48 h and subsequent treatment with 2 mM hydroxyurea for 24 h (Fig. 4). HeLa cells arrested in the G_0 phase (time = 0 h) were treated with serum, causing them to enter the G_1/S phase. During the G_0 phase, DDX3 and DDX5 were localized predominantly in the nucleus. Their nuclear signals overlapped strongly (Fig. 4A–C). DDX3 was maximally expressed in the cytoplasm during the G_1/S phase (from 4 to 10 h; Fig. 4E and I). Cytoplasmic DDX5 levels also increased during the G_1/S phase (Fig. 4F and J). During the S phase, the level of DDX3 in the cytoplasm decreased versus that in the G_1 phase (Fig. 4I vs. Fig. 4M). When the cells entered the M phase (from 12 to 16 h), the nuclear membrane disappeared. DDX3 was localized in the cytoplasm (Fig. 4M and Q) and DDX5 in the condensed chromosomes (Fig. 4R and W). During telophase, DDX3 displayed a gradual increase in expression and localized around the newly synthesized nuclear membrane and in the cytoplasm. At 16 h, the cells had completed cytokinesis and re-entered the G_1 phase, and the two RNA helicases co-localized in the cytoplasm. After mitosis, the cells continued to the next phase of the cell cycle (G_1 phase). At this stage (time = 24 h), DDX3 and DDX5 were highly expressed and co-localized in the cytoplasm.

EFFECT OF PHOSPHATASE TREATMENT ON THE PROTEIN–PROTEIN INTERACTION

Because the phosphorylation patterns of DDX3 and DDX5 changed during the cell cycle, we analyzed the effect of phosphorylation on the interaction between DDX3 and DDX5 using the phosphatases

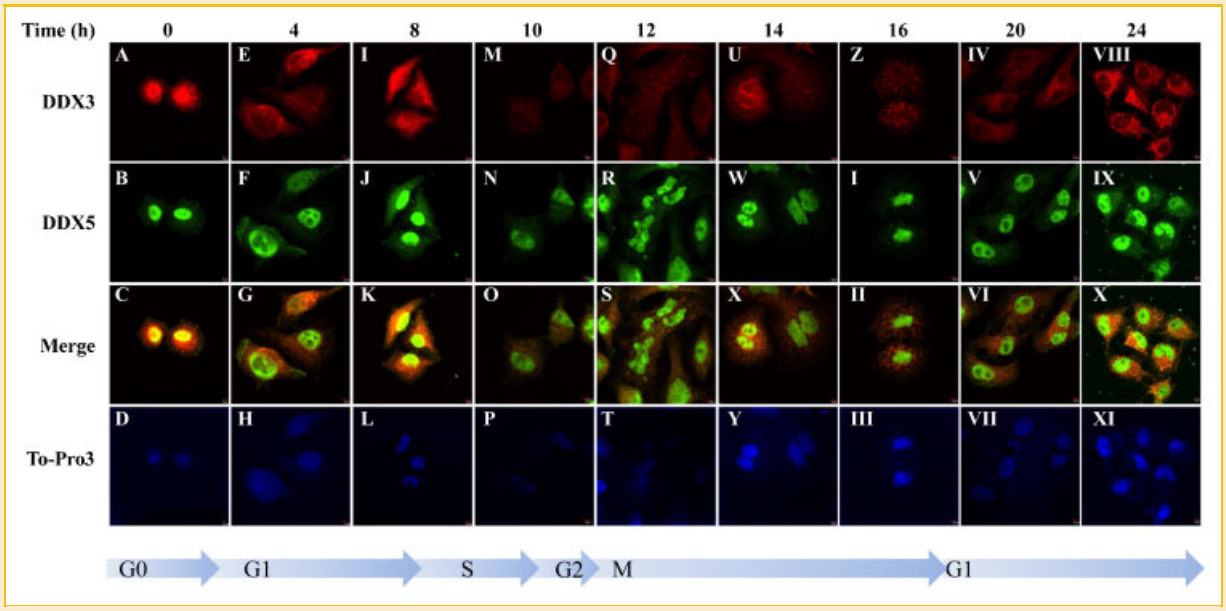

Fig. 4. Localization analysis of DDX3 and DDX5 during the cell cycle. HeLa cells were synchronized by treatment with 2 mM hydroxyurea (Sigma) twice for 12 h to reach the G_1/S phase. For G_2/M phase arrest, HeLa cells were treated with 600 ng/ml nocodazole until all cells became mitotic. Cells were stained with specific antibodies at 2–4 h intervals. The relative localization of proteins was determined by labeling, with appropriate secondary antibodies conjugated to Alexa Fluor 546 (red) and Alexa Fluor 488 (green) being used for DDX3 (A, E, I, M, Q, U, Z, IV, and VIII) and DDX5 (B, F, J, N, R, W, I, V, and VX), respectively. Cell nuclei were stained with TO-PRO-3 (D, H, L, P, T, Y, III, VII, and XI). Stained cells were visualized using a laser confocal scanning microscope. [Color figure can be seen in the online version of this article, available at http://wileyonlinelibrary.com/journal/jcb]

PP2A and PTP1B, and then performed IP with an anti-DDX3 antibody (see Supplementary Fig. 1). When unsynchronized whole cell lysates were treated with PP2A and/or PTP1B, levels of immunoprecipitated DDX3 and DDX5 did not change significantly (Fig. 5A). However, when the cytoplasmic fraction from unsynchronized cells was treated with PP2A, but not PTP1B, the level of immunoprecipitated DDX5 increased (Fig. 5B). In the case of G_2/M phase-arrested cells, treatment of the cytoplasmic fraction with PP2A increased the level of immunoprecipitated DDX5 compared with the untreated control; however, PTP1B and PP2A/PTP1B treatment did not affect the protein–protein interaction (Fig. 5C). To verify the effect of the phosphorylation pattern on protein–protein interactions, Myc-DDX3, and GST-DDX5 were transfected into HEK293 cells, whole cell lysates were treated with PP2A and/or PTP1B, and GST pull-down was performed. At 48 h post-transfection, Myc-DDX3 and GST-DDX5 were analyzed by IP. These tagged proteins were precipitated with the corresponding antibodies (Fig. 6A). Treatment with PP2A or PP2A/PTP1B increased the amount of DDX3 pulled down, whereas, treatment with PTP1B alone did not (Fig. 6B). To confirm the effect of PP2A, the PP2A inhibitor calyculin A was co-administered and GST pull-down was then carried out. Calyculin A treatment reduced the amount of DDX3 pulled down (Fig. 6C). Bacterially expressed His-DDX3 and His-DDX5 were pretreated with PP2A and/or PTP1B, incubated with cytoplasmic lysates from unsynchronized cells, and subjected to IP analysis. PP2A- or PP2A/PTP1B-pretreated His-DDX5 more efficiently interacted with endogenous DDX3 (Fig. 6D). Pretreatment with PP2A or PP2A/PTP1B also increased the interaction of His-DDX3 with endogenous DDX5 (Fig. 6E). These results are in agreement with the protein–protein interaction between endogenous DDX3 and DDX5 (Fig. 5).

INVOLVEMENT OF DDX3 AND DDX5 IN mRNP EXPORT

Previously, DDX3 was shown to regulate mRNP export by interacting with TAP, which is recruited to mRNPs in the nucleus and which participates in their export [Lai et al., 2008]. Furthermore, DDX3 and DDX5 are also known to be components of the mRNP complex formed with spliced mRNAs [Merz et al., 2007]. These mRNP proteins influence all aspects of the subsequent metabolism of mRNAs, including export from the nucleus, translation efficiency, and stability in the cytoplasm [Moore, 2005]. To confirm the involvement of the protein–protein interaction between DDX3 and DDX5 in mRNP export, UV cross-linking was performed in vivo. Immunoblotting of subcellular fractions revealed that NPM largely localized to the nucleus and α-tubulin to the cytoplasm. Following exposure to UV light, DDX3 was co-purified with poly(A) RNAs in both the nucleus and the cytoplasm (Fig. 7A), as described previously [Lai et al., 2008]. DDX5 was largely purified with mRNAs in the nucleus, and only weakly in the cytoplasm. To examine whether DDX3 affected the activity of DDX5 in mRNP export, shDDX3 was transfected into cells to reduce DDX3 expression. UV cross-linking analysis was then performed (Fig. 7B). Interestingly, DDX3 knockdown reduced the level of DDX5 in the nucleus, compared with untransfected control cells, while increasing the level of DDX5 in the cytoplasm. Thus, DDX3 may be involved in the shuttling of DDX5 by the mRNP export machinery.

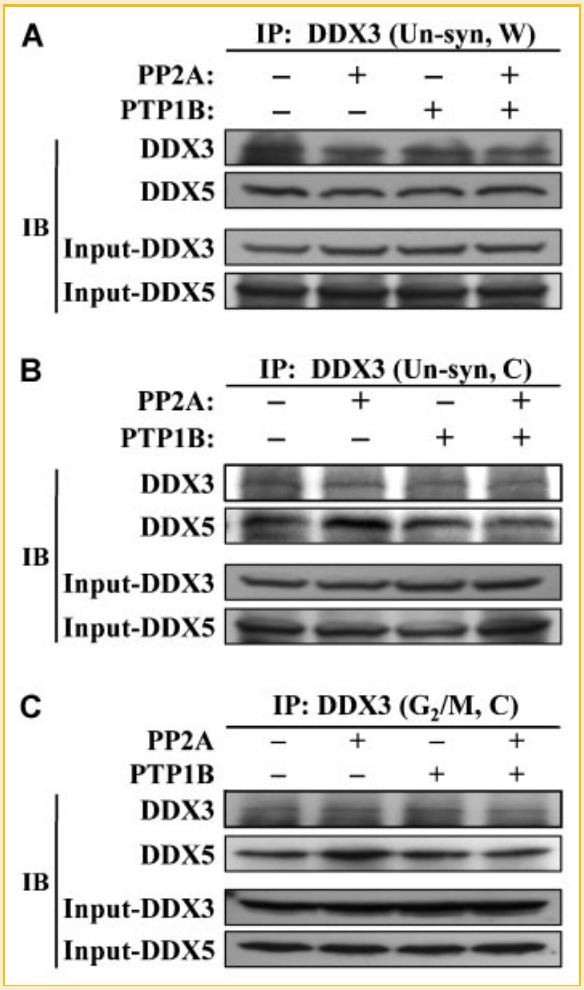

Fig. 5. Effects of phosphatase treatment on the interaction between DDX3 and DDX5. HeLa cell lysates were prepared and 1.5 mg of protein was treated with 0.12 U PP2A and/or 0.19 U PTP1B for 2 h at 30°C. Whole cell lysates (A) or cytoplasmic HeLa cell fractions (B) were treated with PP2A and/or PTP1B and then subjected to IP analysis with an anti-DDX3 antibody. C: To analyze the effects of phosphatase treatment on the interaction between DDX3 and DDX5 during the cell cycle, HeLa cells were synchronized by treatment with 600 ng/ml nocodazole until all cells became mitotic. The cytoplasmic fraction was treated with phosphatase, as described above, and then subjected to IP analysis with an anti-DDX3 antibody.

DISCUSSION

The present study demonstrates that DDX3 interacts with DDX5 and that these proteins are co-localized and co-immunoprecipitated in the cytoplasm. Both proteins are members of the DEAD-box RNA helicase superfamily and share homology in their helicase domains: DDX3 (aa 168–567) has 43% identity and 60% similarity with DDX5 (aa 82–467). The N-terminal and C-terminal regions of DDX3 and DDX5 did not show homology. Using a yeast two-hybrid assay, we identified the interaction between these two DEAD-box RNA helicases. DDX3 interacted with the C-terminal region of DDX5 and vice versa. The C-terminal region of DDX3 (aa 415–662), which contains helicase motifs IV–VI and a Ser/Gly-rich region, interacted with the C-terminal region of DDX5 (aa 373–614), which contains helicase motifs V and VI. The C-terminal region (aa 501–662) of DDX3 contains a Ser/Gly-rich sequence that is separated from the highly conserved RNA helicase domains V–VI and is known to interact with the hepatitis C core protein [Mamiya and Worman, 1999; Owsianka and Patel, 1999; You et al., 1999]. The C-terminal region of DDX5 contains the RGS-RGG motif and the IQ motif. The RGS-RGG motif may resemble a conserved protein sequence found in many RNA-binding proteins and function as an RNA-binding site for DDX5 [Kiledjian and Dreyfuss, 1992; Yang and Liu, 2004]. The IQ motif has a putative phosphorylation site, located within an 85 amino acid segment (aa 528–614) in which none of the amino acid residues is charged under physiological conditions [Yang and Liu, 2004]. Thus, the C-terminal region of DDX5 is a common site of interaction with DDX3 and RNA binding, and this region may thus modulate biological functions by interaction with DDX3 and/or RNA substrate binding.

Interestingly, the intracellular localization and expression level of DDX3 changed with the cell cycle. DDX3 was localized in the nucleus in the G_0 phase, but was predominantly localized in the cytoplasm during the G_1/S phase, which corresponds to biological functions, such as translational control and mRNA transport via mRNP complexes. During the G_2/M phase, the level of DDX3 decreased, as shown by IF and IP analyses. Previously, inactivation of Ded1p, a yeast homolog of DDX3, was shown to cause arrest at the beginning of stage G_1 and at stage G_2, prior to mitosis. At the G_2/M checkpoint, mutation of Ded1p inhibits stress-induced G_2/M transition and cell cycle progression, independent of cdc2 tyrosine phosphorylation [Forbes et al., 1998]. Knockdown of DDX3 with small interfering RNAs results in premature entry into the S phase and enhanced cell growth [Chang et al., 2006]. This enhanced cell cycle progression is linked to the up-regulation of cyclin D1 and the down-regulation of DDX3. In a temperature-sensitive (ts) hamster cell line containing a single-point mutation in Ddx3, ts mutant cells are arrested at the G_1 phase and Ddx3x accumulated in the nucleus at non-permissive temperatures [Fukumura et al., 2003]. In ts mutant cells, general protein synthesis is not strongly inhibited, but rather mRNA and cap-binding protein eIF4E accumulate in the nucleus. Thus, the present data suggest a possibility that the cell cycle may be regulated by the phosphorylation of DDX3 at specific sites or its interaction with partner proteins. However, further study is required to determine the specific phosphorylation sites and target kinases and to assess cell cycle control and biological functions of DDX3.

DDX5 is a known nuclear matrix/chromatin-associated protein that mediates the connections among chromosomes during mitosis [Akileswaran et al., 2001; Cronshaw et al., 2002; Enukashvily et al., 2005]. DDX5 is found in both the centromeric regions and the connections between chromosomes [Enukashvily et al., 2005]. Our IF data show that DDX5 is tightly associated with the chromatin complex during mitosis, and that DDX3 does not interact with DDX5 associated with chromatin but only interacts with cytoplasmic DDX5 (Fig. 4S). The level of nuclear DDX5 in the G_2/M phase was not changed compared with that in the G_1/S phase, or in unsynchronized cells (Fig. 3C). In the IF analysis, DDX5 was consistently stained in the nucleus and did not show any expression changes based on the

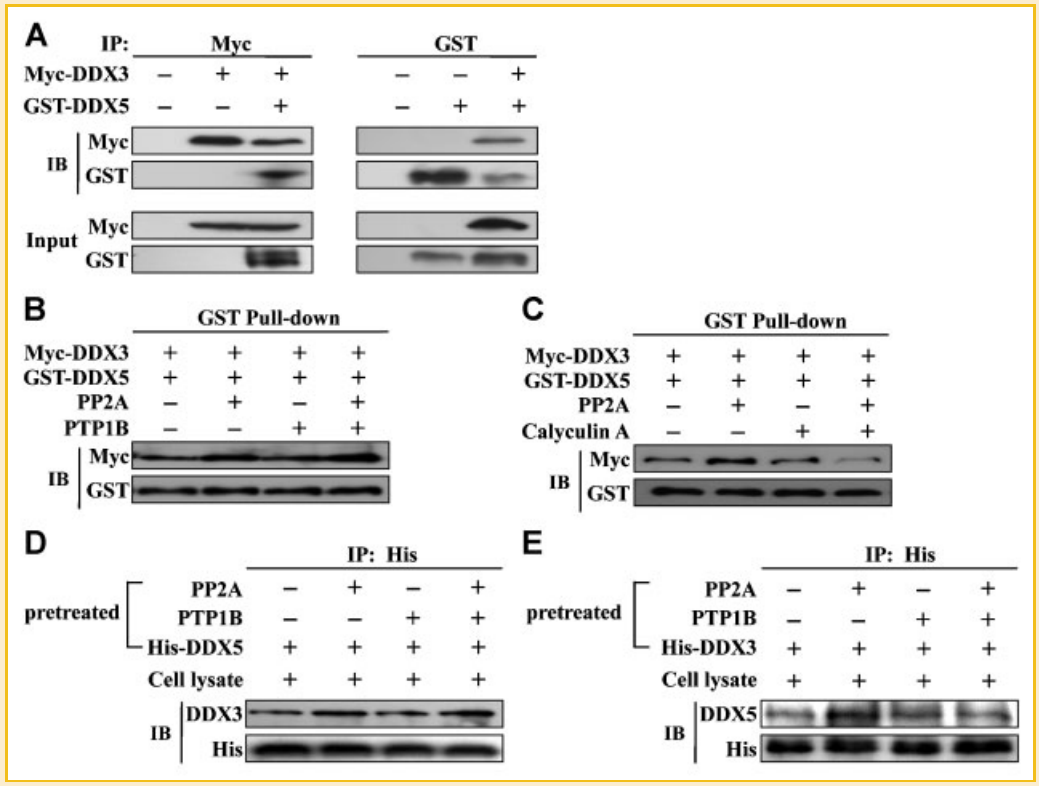

Fig. 6. GST pull-down analysis. A: Myc-DDX3 and GST-DDX5 were transfected into HeLa for 48 h and lysates then immunoblotted with anti-Myc and anti-GST antibodies. B: The transfected cell lysates were treated with 0.12 U PP2A and/or 0.19 U PTP1B for 2 h at 30°C and then incubated with glutathione affinity gels. After centrifugation, the gel was washed with PBS buffer and immunoblotted with anti-Myc and anti-GST antibodies. C: The transfected cell lysates were treated 0.1 μM calyculin A for 30 min on ice and then treated with 0.12 U PP2A for 2 h at 30°C. The mixtures were incubated with glutathione affinity gel and immunoblotted with anti-Myc and anti-GST antibodies. To verify the effects of phosphorylation on the protein–protein interaction, His-DDX5 (D), and His-DDX3 (E) were pre-treated with PP2A and/or PTP1B and then incubated with the cytoplasmic fraction of unsynchronized cells. IP analysis was then performed with an anti-His antibody. Immunoblotting was finally carried out with an anti-DDX3 or anti-DDX5 antibody.

cell cycle. These findings agree with those of previous studies. Immunohistochemical studies of DDX5 expression in a variety of cell lines have shown granular nuclear staining which is generally excluded from the nucleoli in interphase cells [Iggo and Lane, 1989; Nicol et al., 2000]. However, in cells that have recently divided, DDX5 is transiently associated with discrete densely stained bodies that are believed to be prenucleolar bodies [Iggo et al., 1991; Nicol et al., 2000], thus suggesting limited cell-cycle-dependent alteration in nuclear localization. However, the cytoplasmic levels of DDX5 were increased during the G_2/M phase, as was its phosphorylation at serine, threonine, and tyrosine residues. Especially, the increase in cytoplasmic DDX5 level during the M phase may be due to loss of the nuclear membrane (Fig. 4R), an increase in DDX5 expression, or increased DDX5 stability, resulting from its interaction with chromatin and/or phosphorylation. Thus, the protein–protein interaction during the G_2/M phase may be affected by the increase in cytoplasmic DDX5 levels, as well as by the phosphorylation status of both proteins. Dephosphorylation experiments performed using PP2A and/or PTP1B showed that the interaction between the two DEAD-box RNA helicases was greatly affected by PP2A treatment. Notably, PP2A increased the amount of DDX5 precipitated from the cytoplasmic fraction of unsynchronized cells, as well as of G_2/M phase-arrested cells. These data are confirmed by the result of experiment using bacterial recombinant His-DDX3. IP analysis against GST-tagged DDX5 or bacterial recombinant His-DDX5 showed that PP2A and PP2A/PTP1B reduced the interaction with DDX3, suggesting that phosphorylation at serine/threonine residue(s) strongly affected the protein–protein interaction, but phosphorylation at tyrosine residue(s) did not (Fig. 6B,D). However, in the case of DDX3, PP2A increased the protein–protein interaction, but PTP1B or PP2A/PTP1B did not affect the interaction with DDX5. These results indicate that phosphorylation of DDX3 and/or DDX5 at serine/threonine residue(s) negatively affected the protein–protein interaction. DDX3 is phosphorylated at serine/threonine residue(s) by cyclin B/cdc2 [Sekiguchi et al., 2007] or TANK-binding kinase 1 (TBK1) [Soulat et al., 2008], which is associated with a loss in DDX3 function to repress cyclin A expression, decreasing ribosome biogenesis and translation during mitosis, or stimulation of innate immunity against pathogen infection by induction of interferon-β expression. Phosphorylation of DDX5 in the C-terminal domain (aa 431–614) by protein kinase C abolishes its RNA binding [Yang and Liu, 2004]. Since the C-terminal region of DDX5 is perfectly matched with the interacting region with DDX3, we suggest that DDX3 may interact with dephosphorylated DDX5 at serine/

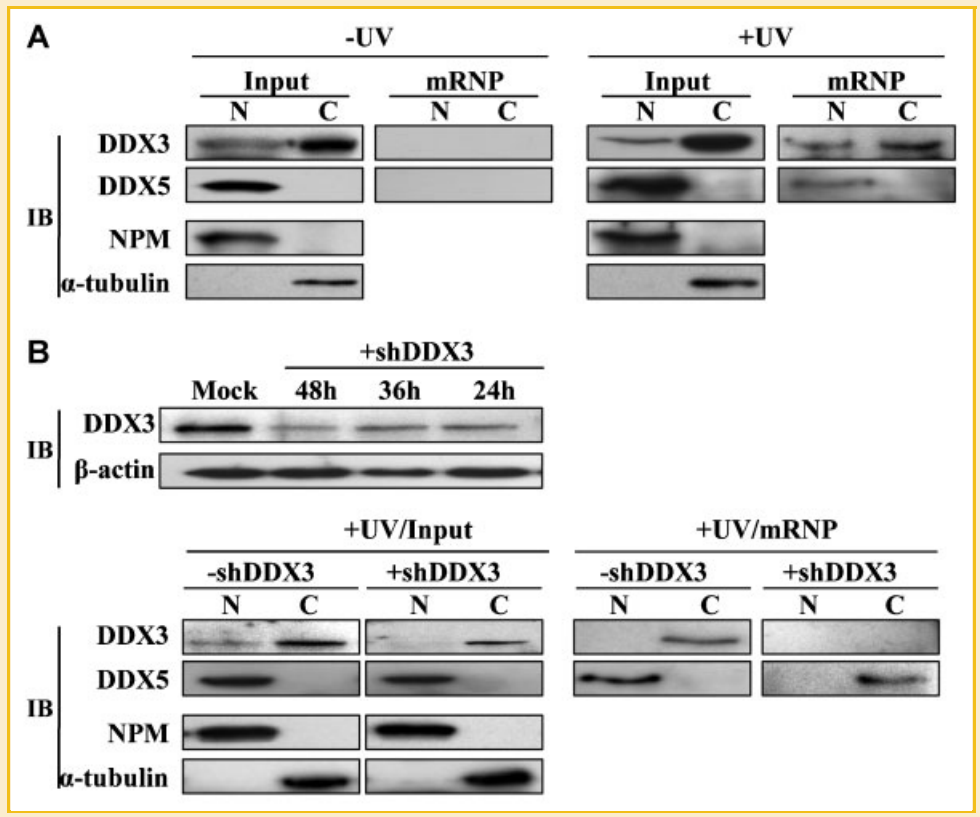

Fig. 7. Involvement of DDX3 and DDX5 in mRNP export. A: UV-radiated (+UV) and untreated control (−UV) HEK293 cells were subjected to cell fractionation. The lysates were then subjected to chromatography on poly(U)-Sepharose. Proteins cross-linked to poly(A)+ RNAs were detected using an anti-DDX3 or anti-DDX5 antibody. The subcellular fractions were also subjected to immunoblotting using antibodies against NPM and α-tubulin. B: shDDX3, which targets DDX3, was transiently transfected into HEK293 cells. Immunoblotting of cell lysates was performed using an anti-DDX3 antibody. UV cross-linking and poly(U)-Sepharose-affinity selection were performed as described above.

threonine residues, which carry the RNA substrate, and may be involved in mRNP export. However, to understand the effects of phosphorylation at serine/threonine residues of both DEAD-box RNA helicase proteins on their interaction and biological roles, further studies are required.

mRNA products generated by splicing are complexed with a currently unknown number of proteins, some of which are deposited as a consequence of splicing. These proteins influence every aspect of subsequent mRNA metabolism, including export from the nucleus, translation efficiency, and stability in the cytoplasm [Moore, 2005]. DDX5 is an essential splicing factor that facilitates unwinding of the U1 snRNA/5′-splice site base-pairs [Liu, 2002]. Consistent with its role in splicing, it has been detected in numerous spliceosomal complexes. DDX3 has also been detected in a mixture of affinity-purified human spliceosomes and mRNPs [Zhou et al., 2002] and spliceosomal B complexes [Deckert et al., 2006]. Furthermore, DDX3 and DDX5 have been detected in splicing-dependent mRNP-associated complexes [Merz et al., 2007]. DDX3 is more stably associated with mRNP complexes following heparin treatment compared with DDX5. After the export of mRNPs into the cytoplasm, exon junction complexes are removed from the mRNA by the ribosome during the first round of translation, and most of the remaining components shuttle back to the cell nucleus [Dostie and Dreyfuss, 2002]. DDX3, a nucleo-cytoplasmic shuttling protein, may be involved in the shuttling of DDX5 to the nucleus. DDX3 knockdown reduced levels of DDX5 in mRNP complexes in the nuclear fraction while increasing its levels in the cytoplasmic fraction. Although we could not confirm a direct interaction between both proteins in an mRNP complex, DDX3 might regulate the shuttling of DDX5 to the nucleus.

Various proteins are known to interact with DDX3, such as several translation initiation factors (eIF4e, eIF4a, eIF2α, PABP, and eIF3), transcription factor SP1, spliced mRNA in an exon junction complex, mRNP complex, nucleo-cytoplasmic shuttling proteins (CRM1 and TAP), and viral proteins (hepatitis B virus DNA polymerase, HCV core protein, and vaccinia virus K7) [see Schröder, 2010]. However, the present study is the first to report that DDX3 interacts with the DEAD-box RNA helicase DDX5. Many previous studies have suggested the possibility of a direct interaction and a functional relationship between DDX3 and DDX5. For example, the two RNA helicases have been detected in intrinsic antiretroviral factor APOBEC3G complexes [Chiu et al., 2006] and in calmodulin (CaM)-associated protein complexes [Jang et al., 2007]. Although many studies have reported the coexistence of DDX3 and DDX5 in RNA metabolism-related complexes, the present study is, to our knowledge, the first report

demonstrating a direct interaction between these proteins. Moreover, their interaction is affected by the phosphorylation states of both proteins and the cell cycle. Furthermore, UV cross-linking analysis indicated that DDX3 and DDX5 are jointly involved in mRNP export and that DDX3 may be required for the shuttling of DDX5 to the nucleus. Our study reveals a novel protein–protein interaction between two DEAD-box RNA helicases and suggests a mechanisms of action of these helicases in mRNP export, including during virus proliferation, cell proliferation, apoptosis, and abnormal cell growth.

ACKNOWLEDGMENTS

We thank for DDX5 cloned plasmids provided by Prof. Fuller-Pace (University of Dundee, Dundee, Scotland, UK). This work was supported by grant No. (R04-2003-000-10126-0) from the Basic Research Program of the Korea Science & Engineering Foundation, Republic of Korea and supported by Priority Research Centers Program through the National Research Foundation of Korea (NRF) funded by the Ministry of Education, Science, and Technology (Project No. 2011-0018393) to S-G Lee.

REFERENCES

Akileswaran L, Taraska JW, Sayer JA, Gettemy JM, Coghlan VM. 2001. A-kinase-anchoring protein AKAP95 is targeted to the nuclear matrix and associates with p68 RNA helicase. J Biol Chem 276:17448–17454.

Arimui Y, Kuroki M, Abe K, Dansako H, Ikeda M, Wakita T, Kato N. 2007. DDX3 DEAD-box RNA helicase is required for hepatitis C virus RNA replication. J Virol 81:13922–13926.

Chang PC, Chi CW, Chau GY, Li FY, Tsai YH, Wu JC, Wu Lee YH. 2006. DDX3, a DEAD box RNA helicase, is deregulated in hepatitis virus-associated hepatocellular carcinoma and is involved in cell growth control. Oncogene 25:1991–2003.

Chiu YL, Witkowska HE, Hall SC, Santiago M, Soros VB, Esnault C, Heidmann T, Greene WC. 2006. High-molecular-mass APOBEC3G complexes restrict Alu retrotransposition. Proc Natl Acad Sci USA 103:15588–15593.

Cronshaw KM, Krutchinsky AN, Zhang W, Chait BT, Mayunis MJ. 2002. Proteomic analysis of the mammalian nuclear pore complex. J Cell Biol 158:915–927.

Deckert J, Hartmuth K, Boehringer D, Behzadnia N, Will CL, Kastner B, Stark H, Urlaub H, Lührmann R. 2006. Protein composition and electron microscopy structure of affinity-purified human spliceosomal B complexes isolated under physiological conditions. Mol Cell Biol 26:5528–5543.

Dostie J, Dreyfuss G. 2002. Translation is required to remove Y14 from mRNAs in the cytoplasm. Curr Biol 12:1060–1067.

Endoh H, Maruyama K, Masuhiro Y, Kabayashi Y, Goto M, Tai H, Yanagisawa J, Metzger D, Hashimoto S, Kato S. 1999. Purification and identification of p68 RNA helicase acting as a transcriptional coactivator specific for the activation function 1 of human estrogen receptor alpha. Mol Cell Biol 19:5363–5372.

Enukashvily N, Donev R, Sheer D, Podgornaya O. 2005. Satellite DNA binding and cellular localisation of RNA helicase p68. J Cell Sci 118:611–622.

Forbes KC, Humphrey T, Enoch T. 1998. Suppressors of cdc25p overexpression identify two pathways that influence the G2/M checkpoint in fission yeast. Genetics 150:1361–1375.

Fukumura J, Noguchi E, Sekiguchi T, Nishimoto T. 2003. A temperature-sensitive mutant of the mammalian RNA helicase, DEAD-box X isoform, DBX, defective in the transition from G1 to S phase. J Biochem 134: 71–82.

Fuller-Pace FV. 2006. DExD/H box RNA helicases: Multifunctional proteins with important roles in transcriptional regulation. Nucleic Acids Res 34: 4206–4215.

Goh PY, Tan YJ, Lim SP, Tan YH, Lim SG, Fuller-Pace F, Hong W. 2004. Cellular RNA helicase p68 relocalization and interaction with the hepatitis C virus (HCV) NS5B protein and the potential role of p68 in HCV RNA replication. J Virol 78:5288–5298.

Iggo RD, Lane DP. 1989. Nuclear protein p68 is an RNA-dependent ATPase. EMBO J 8:1827–1831.

Iggo RD, Jamieson DJ, MacNeill SA, Southgate J, McPheat J, Lane DP. 1991. p68 RNA helicase: Identification of a nucleolar form and cloning of related genes containing a conserved intron in yeasts. Mol Cell Biol 11:1326–1333.

Jang D, Guo M, Wang D. 2007. Proteomic and biochemical studies of calcium- and phosphorylation-dependent calmodulin complexes in mammalian cells. J Proteome Res 6:3718–3728.

Kanai Y, Dohmae N, Hirokawa N. 2004. Kinesin transports RNA: Isolation and characterization of an RNA-transporting granules. Neuron 43:513–525.

Kiledjian M, Dreyfuss G. 1992. Primary structure and binding activity of the hnRNP U protein: Binding RNA through RGG box. EMBO J 11:2655–2664.

Lai MC, Wu Lee YH, Tarn WY. 2008. The DEAD-box RNA helicase DDX3 associates with export messenger ribonucleoproteins as well as tip-associated protein and participates in translational control. Mol Biol Cell 19:3847–3858.

Linder P. 2006. Dead-box proteins: A family affair-active and passive players in RNP-remodeling. Nucleic Acids Res 34:4168–4180.

Liu ZR. 2002. p68 RNA helicase is an essential human splicing factor that acts at the U1 snRNA-5′ splice site duplex. Mol Cell Biol 22:5443–5450.

Mamiya N, Worman HJ. 1999. Hepatitis C virus core protein binds to a DEAD box RNA helicase. J Biol Chem 274:15751–15756.

Merz C, Urlaub H, Will CL, Lührmann R. 2007. Protein composition of human mRNPs spliced in vitro and differential requirements for mRNP protein recruitment. RNA 13:116–128.

Moore MJ. 2005. From the birth to death: The complex lives of eukaryotic mRNAs. Science 309:1514–1518.

Nicol SM, Causevic M, Prescott AR, Fuller-Pace FV. 2000. The nuclear DEAD box RNA helicase p68 interacts with the nucleolar protein fibrillarin and colocalizes specifically in nascent nucleoli during telophase. Exp Cell Res 257:272–280.

Ogilvie VC, Wilson BJ, Nicol SM, Morrice NA, Saunders LR, Barber GN, Fuller-Pace FV. 2003. The highly related DEAD box RNA helicases p68 and p72 exist as heterodimers in cells. Nucleic Acid Res 31:1470–1480.

Owsianka AM, Patel AH. 1999. Hepatitis C virus core protein interacts with a human DEAD box protein DDX3. Virology 257:330–340.

Piñol-Roma S, Adam SA, Choi YD, Dreyfuss G. 1989. Ultraviolet-induced cross-linking of RNA to proteins in vivo. Methods Enzymol 180:410–418.

Rosner A, Rinkevich B. 2007. The DDX3 subfamily of the DEAD box helicases: Divergent roles as unveiled by studying different organisms and in vitro assays. Curr Med Chem 14:2517–2525.

Salzman DW, Shubert-Coleman J, Furneaux H. 2007. p68 RNA helicase unwinds the human let-7 microRNA precursor duplex and is required for let-7 directed silencing of gene expression. J Biol Chem 282:32773–32779.

Schröder M. 2010. Human DEAD-box protein 3 has multiple functions in gene regulation and cell cycle control ad is primer target for viral manipulation. Biochem Pharmacol 79:297–306.

Schröder M, Baran M, Bowie AG. 2008. Viral targeting of DEAD box protein 3 reveals its role in TBK1/IKKepsilon-mediated IRF activation. EMBO J 27: 2147–2157.

Sekiguchi T, Kurihara Y, Fukumura J. 2007. Phosphorylation of threonine 204 of DEAD-box RNA helicase DDX3 by cyclin B/cdc2 in vitro. Biochem Biophys Res Commun 356:668–673.

Soulat D, Bürckstümmer T, Westermayer S, Goncalves A, Bauch A, Stefanovic A, Hantschel O, Bennett KL, Decker T, Superti-Furga G. 2008. The DEAD-box helicase DDX3X is a critical component of the TANK-binding kinase-1-dependent innate immune response. EMBO J 27:2135–2146.

Yang Y, Liu ZR. 2004. Bacterially expressed recombinant p68 RNA helicase is phosphorylated on serine, threonine, and tyrosine residues. Protein Expr Purif 35:327–333.

Yang Y, Lin C, Liu ZR. 2005. Phosphorylations of DEAD box p68 RNA helicase are associated with cancer development and cell proliferation. Mol Cancer Res 3:355–363.

Yedavalli VS, Neuveut C, Chi YH, Kleiman L, Jeang KT. 2004. Requirement of DDX3 DEAD box RNA helicase for HIV-1 Rev-RRE export function. Cell 119:381–392.

You LR, Chen CM, Yeh TS, Tsai TY, Mai RT, Lin CH, Lee YW. 1999. Hepatitis C virus core protein interacts with cellular putative RNA helicase. J Virol 73:2841–2853.

Zhou Z, Licklider LJ, Gygi SP, Reed R. 2002. Comprehensive proteomic analysis of the human spliceosome. Nature 419:182–185.